26 May 2010, 4:45 pm - 6:45 pm

# A Simple Numerical Tool for Dynamic Soil-Structure Interaction Analyses Including Non-Linear Behaviour of Both Structure and Foundation

R. Figini

*Politecnico di Milano, Italy*

C. T. Chatzigogos

*Géodynamique et Structures, France*

R. Paolucci

*Politecnico di Milano, Italy*

Fifth International Conference on
Recent Advances in Geotechnical Earthquake Engineering and Soil Dynamics
*and Symposium in Honor of Professor I.M. Idriss*
May 24-29, 2010 • San Diego, California

# A SIMPLE NUMERICAL TOOL FOR DYNAMIC SOIL-STRUCTURE INTERACTION ANALYSES INCLUDING NON-LINEAR BEHAVIOUR OF BOTH STRUCTURE AND FOUNDATION

**R. Figini**
Politecnico di Milano,
Milano, Italy

**C. T. Chatzigogos**
Géodynamique et Structures,
Bagneux, France

**R. Paolucci**
Politecnico di Milano
Milano, Italy

ABSTRACT

In this paper a simple model to take into account dynamic non-linear soil-structure interaction is presented: it consists of a 1 degree-of-freedom (dof) superstructure and a 3 dof macro-element foundation. Both the superstructure and the soil-foundation system exhibit a non-linear behaviour. In particular the superstructure is characterized by an elastic perfectly plastic behaviour, while the foundation macro-element encompasses the two sources of non-linearity that arise in the soil-foundation interface: a) the one due to the irreversible elastoplastic soil behaviour (material non-linearity) and b) the one due to possible foundation uplift (geometric non-linearity). The global model thus entails the following features: a) the coupling between the foundation and the superstructure when one or both of them enter into the non-linear range, b) the capability for the foundation and the superstructure to dissipate energy, c) a prediction of peak and residual displacements in both the superstructure and the foundation, d) the possibility to model the isolation effects for the structure due to the foundation non-linear behaviour and e) the possibility for the superstructure to reach a particular level of ductility demand. Therefore, the model can serve as a numerical tool for assessing performance-based design approaches that wish to take into account non-linear soil-structure interaction. This is illustrated through several case studies of bridge piers, in which a comparison between the results obtained by dynamic analyses performed with different base conditions (fixed base, elastic base, elastoplastic base with uplift) emphasizes the role of the non-linear soil-structure interaction in design.

## INTRODUCTION

In the contest of earthquake-resistant design of structures it has been widely recognized that a design in which the structure remains linear is in most cases financially unaffordable. This has motivated performance-based design methods, in which a certain level of non-linear response is acceptable during a seismic excitation as long as the performance of the structure complies with certain predefined design criteria. So, on one hand, the consideration of the various sources of non-linearity in the global structure-foundation-soil system becomes indispensable for design. On the other hand, this complicates significantly the modeling process and requires tools that may be far beyond conventional computational capacities. For these reasons, engineering practice has privileged the development of simplified models describing the non-linearities in a structure subjected to earthquake loading. Classical earthquake engineering design considers the non-linearity to develop in the superstructure alone. However, another important source of non-linearity, that is commonly neglected, is concentrated at the soil-foundation level. For rigid shallow footings in particular, many simplified models have been proposed, most of which belonging to the so-called “macro-element” type: in these models the entire soil-footing system is replaced by a single macro-element placed at the base of the structure and aiming at reproducing the non-linear effects arising at the soil-footing interface. Applications of the macro-element have been presented so far mostly for linear superstructure behaviour (Paolucci, 1997; Cremer *et al.*, 2001; Chatzigogos, 2007; Paolucci *et al.*, 2008). The scope of the present paper is to propose a simplified numerical tool in which non-linearities can develop both at the superstructure and at the soil-footing level. After a presentation of the main features of this numerical tool, we describe the macro-element models implemented in it. Then we discuss some results from analyses performed on bridge piers, trying to underline the capabilities of the tool, as well as possible implications of non-linear soil-structure interaction effects on performance based design procedures.

DESCRIPTION OF THE NUMERICAL TOOL

Mathematical formulation

A complete and rigorous approach to the dynamic soil-structure interaction problem would be the global modelling of the soil-foundation-superstructure system by dynamic finite element analyses. This approach requires large scale computations and delicate solution techniques. On the other hand, the need to perform parametric studies due to the stochastic nature of input motion motivates the development of simplified numerical models, that can both capture the salient features of the coupling between the non-linear response of the soil-foundation system and the non-linear superstructure, and reduce the overall computational cost. To this end, a simplified model of a single degree-of-freedom (dof) structure, resting on a three dof shallow foundation (horizontal and vertical motion, plus rocking around its centre of mass) has been considered (Fig. 1).

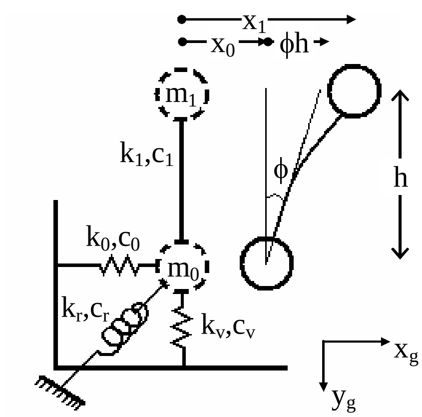


*Fig.1. Four dof model for soil-structure interaction analyses (Paolucci , 1997, Paolucci et al., 2008)*

This model was originally proposed by Paolucci (1997), assuming a linear behaviour of the superstructure and an elastic perfectly plastic behaviour for the soil-foundation macro-element. The original mathematical formulation has been slightly modified herein to introduce non-linearity in the superstructure level as well. The dynamic equilibrium of the system in Fig. 1 is described by the following set of equations:

$$\underline{\underline{\boldsymbol{M}}}\,\underline{\ddot{\boldsymbol{x}}} + \underline{\underline{\boldsymbol{C}}}\,\underline{\dot{\boldsymbol{x}}} + \underline{\boldsymbol{F}}^{\boldsymbol{S}} + \underline{\boldsymbol{F}}^{\boldsymbol{F}} = \underline{\boldsymbol{p}} \qquad (1)$$

where

$$\underline{\boldsymbol{x}} = \begin{bmatrix} \boldsymbol{x}_1 & \boldsymbol{x}_0 & \boldsymbol{\phi} & \boldsymbol{x}_{\boldsymbol{v}} \end{bmatrix}^{\boldsymbol{T}};$$

$$\underline{\boldsymbol{F}}^{\boldsymbol{S}} = \begin{bmatrix} \boldsymbol{V}^{\boldsymbol{S}} & -\boldsymbol{V}^{\boldsymbol{S}} & -\boldsymbol{V}^{\boldsymbol{S}}\boldsymbol{h} & 0 \end{bmatrix}^{\boldsymbol{T}};$$

$$\underline{\boldsymbol{F}}^{\boldsymbol{F}} = \begin{bmatrix} 0 & \boldsymbol{V}^{\boldsymbol{F}} & \boldsymbol{M}^{\boldsymbol{F}} & \boldsymbol{N}^{\boldsymbol{F}} \end{bmatrix}^{\boldsymbol{T}};$$

$$\underline{\boldsymbol{p}} = \begin{bmatrix} -\boldsymbol{m}_1\ddot{\boldsymbol{x}}_{\boldsymbol{g}} & -\boldsymbol{m}_0\ddot{\boldsymbol{x}}_{\boldsymbol{g}} & 0 & -(\boldsymbol{m}_1+\boldsymbol{m}_0)\ddot{\boldsymbol{y}}_{\boldsymbol{g}} \end{bmatrix}^{\boldsymbol{T}};$$

$$\underline{\underline{\boldsymbol{M}}} = \begin{bmatrix} \boldsymbol{m}_1 & 0 & 0 & 0 \\ 0 & \boldsymbol{m}_0 & 0 & 0 \\ 0 & 0 & \boldsymbol{J} & 0 \\ 0 & 0 & 0 & \boldsymbol{m}_1+\boldsymbol{m}_0 \end{bmatrix};$$

$$\underline{\underline{\boldsymbol{C}}} = \begin{bmatrix} \boldsymbol{c}_1 & -\boldsymbol{c}_1 & -\boldsymbol{c}_1\boldsymbol{h} & 0 \\ -\boldsymbol{c}_1 & \boldsymbol{c}_1+\boldsymbol{c}_0 & \boldsymbol{c}_1\boldsymbol{h} & 0 \\ -\boldsymbol{c}_1\boldsymbol{h} & \boldsymbol{c}_1\boldsymbol{h} & \boldsymbol{c}_1\boldsymbol{h}^2+\boldsymbol{c}_{\boldsymbol{r}} & 0 \\ 0 & 0 & 0 & \boldsymbol{c}_{\boldsymbol{v}} \end{bmatrix};$$

The following notations are used:

- $x_1$, $x_0$, $\Phi$, $x_v$ = horizontal displacement of the structure, horizontal displacement, rotation and vertical displacement of the foundation;
- $\ddot{x}_g, \ddot{y}_g$ = horizontal and vertical component of ground acceleration;
- $m_1$ = effective mass of the first mode of vibration of the superstructure;
- $m_0$ = mass of the foundation;
- $J$ = sum of the centroidal moments of inertia of the superstructure and of the foundation;
- $h$ = effective height of the first mode of vibration of the superstructure;
- $c_1$, $c_0$, $c_r$, $c_v$ = damping of the superstructure, equivalent dashpot coefficients of the soil-foundation system corresponding to the translational, rocking and vertical modes of vibration;
- $V^S$ = shear transmitted by the superstructure;
- $V^F$, $M^F$, $N^F$ = soil reactions, horizontal , rotational and vertical, respectively.

Note that the vector of the restoring forces of the system has been splitted into two parts: the one relative to the superstructure $\underline{F}^S$, and the other relative to the soil-fondation $\underline{F}^F$. Each of the two components of the system can be considered as a separate element, and described by an appropriate constitutive law. In this way a non-linear behaviour can be implemented also for the superstructure. The solution of system (1) is obtained at each time step through the well-known Newmark time integration scheme as follows:

$$\left(\frac{\underline{\underline{\boldsymbol{M}}}}{\boldsymbol{\beta}\Delta\boldsymbol{t}^2} + \frac{\underline{\underline{\boldsymbol{C}}}\boldsymbol{\gamma}}{\boldsymbol{\beta}\Delta\boldsymbol{t}}\right)\Delta\underline{\boldsymbol{x}}_{\boldsymbol{n}+1} + \Delta\underline{\boldsymbol{F}}^{\boldsymbol{S}}_{\boldsymbol{n}+1} + \Delta\underline{\boldsymbol{F}}^{\boldsymbol{F}}_{\boldsymbol{n}+1} =$$
$$\underline{\boldsymbol{p}}_{\boldsymbol{n}+1} + \underline{\underline{\boldsymbol{M}}}\left(\frac{1-2\boldsymbol{\beta}}{2\boldsymbol{\beta}}\underline{\ddot{\boldsymbol{x}}}_{\boldsymbol{n}} + \frac{1}{\boldsymbol{\beta}\Delta\boldsymbol{t}}\underline{\dot{\boldsymbol{x}}}_{\boldsymbol{n}}\right) + \qquad (2)$$
$$\underline{\underline{\boldsymbol{C}}}\left[\left(\frac{\boldsymbol{\gamma}}{2\boldsymbol{\beta}}-1\right)\underline{\ddot{\boldsymbol{x}}}_{\boldsymbol{n}}\Delta\boldsymbol{t} + \left(\frac{\boldsymbol{\gamma}}{\boldsymbol{\beta}}-1\right)\underline{\dot{\boldsymbol{x}}}_{\boldsymbol{n}}\right]$$

where $\Delta t$ is time step, $\beta = 0.25$ and $\gamma = 0.5$ are the Newmark integration parameters, and the subscript $n$ denotes the generic time step. At the right hand side of Eq. (2) only known quantities are present. Assuming a non-linear behaviour for both the superstructure and the foundation, a system of non-linear equations has to be solved iteratively to derive the unknown vector of displacement increment $\Delta \underline{x}_{n+1}$. The modified (constant stiffness) Newton-Raphson method has been used for this purpose; it is summarized in the following steps:

- an elastic prediction $\Delta \underline{x}^{\,j}$ is made considering $\Delta \underline{F}^{S,j} = \underline{\underline{K}}^{S} \Delta \underline{x}^{j}$ and $\Delta \underline{F}^{F,j} = \underline{\underline{K}}^{F} \Delta \underline{x}^{j}$, where

$$\underline{\underline{K}}^{S} = \begin{bmatrix} k_1 & -k_1 & -k_1 h & 0 \\ -k_1 & k_1 & k_1 h & 0 \\ -k_1 h & k_1 h & k_1 h^2 & 0 \\ 0 & 0 & 0 & 0 \end{bmatrix}$$

$$\underline{\underline{K}}^{F} = \begin{bmatrix} 0 & 0 & 0 & 0 \\ 0 & k_0 & 0 & 0 \\ 0 & 0 & k_r & 0 \\ 0 & 0 & 0 & k_v \end{bmatrix}$$

  are the elastic stiffness matrices of the superstructure and of the soil-foundation, respectively; $k_1$, $k_0$, $k_r$, $k_v$ are the elastic stiffness of the structure, and the translational, rotational and vertical elastic impedances of the soil-foundation system, respectively. The system of equations (2) can be rewritten as $\underline{\underline{A}} \Delta \underline{x}^{j} = \underline{\psi}^{j}$, where $\underline{\underline{A}} = \left( \frac{\underline{\underline{M}}}{\beta \Delta t^2} + \frac{\underline{\underline{C}}\gamma}{\beta \Delta t} + \underline{\underline{K}}^{S} + \underline{\underline{K}}^{F} \right)$ and

$$\underline{\psi}^{j} = \underline{p}_{n+1} + \underline{\underline{M}} \left( \frac{1-2\beta}{2\beta} \ddot{\underline{x}}_n + \frac{1}{\beta \Delta t} \dot{\underline{x}}_n \right) + \underline{\underline{C}} \left[ \left( \frac{\gamma}{2\beta} - 1 \right) \ddot{\underline{x}}_n \Delta t + \left( \frac{\gamma}{\beta} - 1 \right) \dot{\underline{x}}_n \right]$$

- a local correction of force increments is made, based on the constitutive behaviour of each element of the system: $\Delta \underline{F}^{S,j}_{corr}, \Delta \underline{F}^{F,j}_{corr}$ are the correct force increments corresponding to the current displacement increment $\Delta \underline{x}^{\,j}$.
- a new residual is calculated as:

$$\underline{\psi}^{j+1} = \underline{\psi}^{j} - \Delta \underline{F}^{S,j}_{corr} - \Delta \underline{F}^{F,j}_{corr} - \left( \frac{\underline{\underline{M}}}{\beta \Delta t^2} + \frac{\underline{\underline{C}}\gamma}{\beta \Delta t} \right) \Delta \underline{x}^{j}$$

- the convergence on the residual is checked. If it is not satisfied, a new iteration is made restarting from the first point, and estimating a new displacement increment $\Delta \underline{x}^{\,j+1}$.

At the end of the Newton-Raphson iterations the total displacement increment $\Delta \underline{x}_{n+1}$ is calculated summing all the displacement increments $\Delta \underline{x}^{\,j}$: $\Delta \underline{x}_{n+1} = \sum_j \Delta \underline{x}^{j}$. The displacements at time step $n$+1 are finally determined as $\underline{x}_{n+1} = \underline{x}_n + \Delta \underline{x}_{n+1}$.

The elastic perfectly plastic macro-element

Paolucci (1997) used an elastic perfectly plastic macro-element model for shallow strip footings on granular soils in drained conditions, where the elastic response is defined in terms of the dynamic impedances introduced in the previous section. Owing to the simplicity of the analytical expressions and the good agreement with the experimental results for shallow strip footings on dry sand under general planar loading conditions, the yield function $f(\underline{F})$ proposed by Nova and Montrasio (1991) is employed:

$$f(\underline{F}) = v^2 + m^2 + n^2 (1-n)^{2\varsigma} \tag{3}$$

where $v = V / \mu N_{max}$, $m = M / \psi B N_{max}$, $n = N / N_{max}$ are the normalized soil reactions, $N_{max}$ is the ultimate static bearing capacity under vertical centered load, and $\mu$, $\psi$, $\zeta$ are model parameters, whose values are discussed in the quoted paper and in Paolucci *et al.* (2008). A 3D view of the yield function (3) in the $v$, $m$, $n$ space is given in Fig. 2. For the calculation of inelastic displacements and rotations, we make reference to the latest version of the Paolucci model (Paolucci *et al.*, 2008), which adopts the non-associative plastic flow rule proposed by Cremer *et al.* (2002):

$$g(\underline{F}) = \lambda^2 v^2 + \chi^2 m^2 + n^2 \tag{4}$$

The optimum parameters $\lambda = 4$ and $\chi = 6$ were selected, consistent with those employed by Cremer *et al.* (2002).

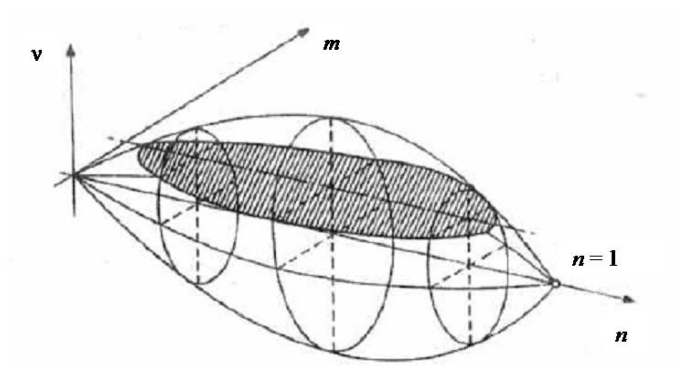


*Fig.2. 3D view of the yield function by Nova and Montrasio (1991)*

The elasto-plastic-uplift macro-element

Chatzigogos (2007) originally proposed a macro-element model for shallow circular footings on cohesive soils.

Chatzigogos and Figini (2008) generalized the original formulation presenting a macro-element model for both circular and strip shallow foundations, encompassing the majority of soil and foundation-soil interface conditions. These include both cohesive and frictional soils, two-dimensional or three-dimensional foundation geometries and interface conditions allowing for foundation uplift or not. The basic idea of the formulation is to depart from the assumption that the surface of ultimate loads of the foundation is identified as a yield surface of a global plasticity model for the soil-footing system. The ultimate surface of the foundation is instead obtained as a combined result of different non-linear mechanisms (soil plasticization, uplift, sliding). The main idea of the model is to describe independently each non-linear mechanism and to retrieve the surface of ultimate loads as the combined result of all active mechanisms. The model includes three non-linear mechanisms: a) sliding along the soil-footing interface, b) plasticization at the vicinity of the footing because of the soil irreversible behaviour and c) the footing uplift. The Chatzigogos macro-element is formulated in terms of dimensionless parameters; dimensionless forces are assembled into the vector $\underline{Q}$ and dimensionless displacements into the vector $\underline{q}$ as follow:

$$\underline{\boldsymbol{Q}}^{\boldsymbol{T}} = [\boldsymbol{Q_N} \quad \boldsymbol{Q_V} \quad \boldsymbol{Q_M}] = \frac{1}{\boldsymbol{aN}_{\max}}[\boldsymbol{aN} \quad \boldsymbol{aV} \quad \boldsymbol{M}] \tag{5}$$

$$\underline{\boldsymbol{q}}^{\boldsymbol{T}} = [\boldsymbol{q_N} \quad \boldsymbol{q_V} \quad \boldsymbol{q_M}] = \frac{1}{\boldsymbol{a}}[\boldsymbol{x_v} \quad \boldsymbol{x}_0 \quad \boldsymbol{a\phi}]$$

where $a$ is the dimension of the footing (width $B$ for strip footings, or diameter $D$ for circular footings). In the following we briefly describe the models adopted for the three mentioned non-linear mechanisms.

*Uplift mechanism*. The uplift mechanism is described by a non-linear elastic model that respects its reversible and non-dissipative character. In fact, footing detachment introduces a non-linearity of geometric nature: as the footing is uplifted, the soil-footing contact area is reduced, which reduces the impedances of the foundation. This is reproduced phenomenologically through a tangent elastic stiffness matrix, function of the level of elastic displacements of the system:

$$\underline{\dot{\boldsymbol{Q}}} = \underline{\underline{\boldsymbol{K}}}\left(\underline{\boldsymbol{q}}^{\boldsymbol{el}}\right)\underline{\dot{\boldsymbol{q}}} \tag{6}$$

The tangent elastic stiffness matrix $\underline{\underline{K}}(\underline{q}^{el})$ is determined through finite element analyses for strip footings (presented by Crémer *et al*. (2001), (2002)) and circular footings (presented by Wolf (1988) and Wolf and Song (2002)). The following assumptions are introduced: *a*) uplift has no effect on the horizontal translation degree-of-freedom of the footing (*cf*. Crémer et al. (2001), (2002)), *b*) the impedance of the footing under vertical load only remains constant during uplift and *c*) for dynamic loading, the dependence of $\underline{\underline{K}}$ on the frequency of excitation is not coupled with its dependence on $\underline{q}^{el}$. Assumptions *a*) and *b*), together with the aforementioned numerical results (Crémer *et al*. (2001), (2002)), lead to the following tangent elastic stiffness matrix describing uplift on an elastic soil:

$$\begin{pmatrix} \dot{\boldsymbol{Q}}_{\boldsymbol{N}} \\ \dot{\boldsymbol{Q}}_{\boldsymbol{V}} \\ \dot{\boldsymbol{Q}}_{\boldsymbol{M}} \end{pmatrix} = \begin{bmatrix} \boldsymbol{K_{NN}} & 0 & \boldsymbol{K_{NM}} \\ 0 & \boldsymbol{K_{VV}} & 0 \\ \boldsymbol{K_{MN}} & 0 & \boldsymbol{K_{MM}} \end{bmatrix} \begin{pmatrix} \dot{\boldsymbol{q}}_{\boldsymbol{N}} \\ \dot{\boldsymbol{q}}_{\boldsymbol{V}} \\ \dot{\boldsymbol{q}}_{\boldsymbol{M}} \end{pmatrix} \tag{7}$$

with elements defined by the following relationships:

$$\boldsymbol{K_{NN}} = \boldsymbol{k_v} \tag{8}$$

$$\boldsymbol{K_{VV}} = \boldsymbol{k}_0$$

$$\boldsymbol{K_{NM}} = \boldsymbol{K_{MN}} = 0 \qquad \text{if } \left|\boldsymbol{q}_{\boldsymbol{M}}^{\boldsymbol{el}}\right| \le \left|\boldsymbol{q}_{\boldsymbol{M},0}^{\boldsymbol{el}}\right|$$

$$\boldsymbol{K_{NM}} = \boldsymbol{K_{MN}} = \boldsymbol{\varepsilon K_{NN}}\left(1 - \frac{\boldsymbol{q}_{\boldsymbol{M},0}^{\boldsymbol{el}}}{\boldsymbol{q}_{\boldsymbol{M}}^{\boldsymbol{el}}}\right) \qquad \text{if } \left|\boldsymbol{q}_{\boldsymbol{M}}^{\boldsymbol{el}}\right| > \left|\boldsymbol{q}_{\boldsymbol{M},0}^{\boldsymbol{el}}\right|$$

$$\boldsymbol{K_{MM}} = \boldsymbol{k_r} \qquad \text{if } \left|\boldsymbol{q}_{\boldsymbol{M}}^{\boldsymbol{el}}\right| \le \left|\boldsymbol{q}_{\boldsymbol{M},0}^{\boldsymbol{el}}\right|$$

$$\begin{aligned} \boldsymbol{K_{MM}} &= \boldsymbol{\gamma\delta K_{MM}}\left(\frac{\boldsymbol{q}_{\boldsymbol{M},0}^{\boldsymbol{el}}}{\boldsymbol{q}_{\boldsymbol{M}}^{\boldsymbol{el}}}\right)^{\delta+1} \\ &+ \boldsymbol{\varepsilon}^2\boldsymbol{K_{NN}}\left(1 - \frac{\boldsymbol{q}_{\boldsymbol{M},0}^{\boldsymbol{el}}}{\boldsymbol{q}_{\boldsymbol{M}}^{\boldsymbol{el}}}\right)^2 \end{aligned} \qquad \text{if } \left|\boldsymbol{q}_{\boldsymbol{M}}^{\boldsymbol{el}}\right| > \left|\boldsymbol{q}_{\boldsymbol{M},0}^{\boldsymbol{el}}\right|$$

$$\boldsymbol{q}_{\boldsymbol{M},0}^{\boldsymbol{el}} = \pm\frac{\boldsymbol{Q_N}}{\boldsymbol{\alpha K_{MM}}} \tag{9}$$

The quantity $\boldsymbol{q}_{\boldsymbol{M},0}^{\boldsymbol{el}}$ represents the rotation angle of the foundation at the moment of uplift initiation. For an elastic soil, this quantity is linear with respect to the applied vertical force on the foundation. The parameters $\alpha$, $\beta$, $\gamma$, $\delta$, $\varepsilon$ are numerical parameters that depend on footing geometry (Chatzigogos and Figini, 2008). We note also that total detachment of the footing is not covered by the present model. Finally, assumption c) is introduced to allow using $\underline{\underline{K}}(\underline{q}^{el})$ for dynamic loading without changing the relationships (8).

*Soil plasticity mechanism.* The soil plasticity mechanism is described through a bounding surface hypoplastic model (Dafalias and Hermann, 1982). The yield surface of classical plasticity is replaced by a bounding surface $f_{BS}$: in the interior of this surface a continuous plastic response is obtained as a function of the distance between the actual force state $Q$ and an image point $\mathbf{I}(Q)$ on the bounding surface, defined through an appropriately chosen mapping rule (Chatzigogos *et al.*, 2008). As the bounding surface is approached, the plastic response becomes more and more pronounced until a plastic flow is eventually produced when the actual force reaches the bounding surface: this situation corresponds to bearing capacity failure of the foundation. We can thus identify the bounding surface $f_{BS}$ with the ultimate surface of a footing resting on a cohesive soil with a perfectly bonded interface (no uplift or sliding allowed). Gouvernec (2007a, 2007b) has presented numerical results offering a detailed determination of this surface for various footing shapes. An approximation sufficient for practical applications and very simple is obtained by considering that the ultimate surface is an ellipsoid centered at the origin:

$$f_{BS} = Q_N^2 + \left(\frac{Q_M}{Q_{M,\max}}\right)^2 + \left(\frac{Q_V}{Q_{V,\max}}\right)^2 - 1 = 0 \qquad (10)$$

The functional form (10) remains approximately independent of footing geometry and soil heterogeneity. The only parameters that change are $Q_{V,max}$ and $Q_{M,max}$, which define the maximum horizontal force and moment respectively: they occur for a zero vertical force. The quantity $N_{max}$ is retrieved from solutions presented by Salençon and Matar (1982). $Q_{V,max}$ is obtained by the condition of sliding along the interface. Finally, $Q_{M,max}$ is obtained for strip footings from solutions presented by Bransby and Randolph (1998) and for circular footings by Gouvernec (2007b).

*Sliding mechanism.* In case of frictional interface, sliding of the footing is induced when the Mohr-Coulomb criterion is violated. The presence of a frictional interface induces a coupling between the three non-linear mechanisms in the system: a) sliding of the footing if the Mohr-Coulomb criterion on the interface is violated, b) uplift of the footing, which is intrinsic in the Mohr-Coulomb interface criterion and c) soil plasticity. When passing to the macro-element scale, the sliding mechanism will induce the two Mohr-Coulomb branches in the $Q_N$-$Q_V$ space, as it is shown in Fig. 3. The global domain of admissible force states will thus be obtained by the intersection of the bounding surface and the Mohr-Coulomb branches, which is convex but non-smooth (see Fig. 3).

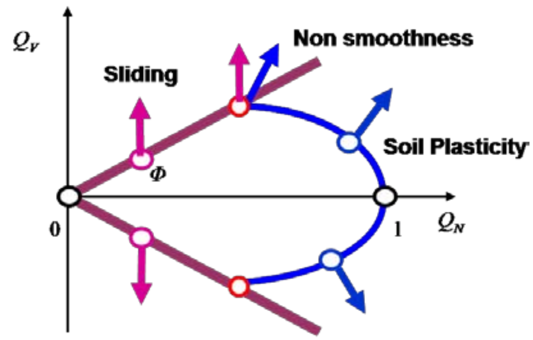


*Fig.3. Coupling between sliding and plasticity in the $Q_N$-$Q_V$ plane*

Non-smoothness can be treated within the multi-mechanism plasticity framework as developed by Koiter (1960) and Mandel (1965). For the examined case, two plastic mechanisms are introduced: the associated bounding surface hypoplastic model presented above and a non-associated perfectly plastic model for the sliding of the footing. For the numerical implementation of multi-mechanism plasticity the algorithm developed by Prévost and Keane (1990) is used. In parallel, the Mohr-Coulomb interface criterion will lead to uplift of the footing on an elastoplastic soil, also with zero dissipation. We can thus implement the non-linear elastic model presented above with the difference that uplift initiation will no longer be linear with respect to $Q_N$ because of the coupling with soil plasticity, as it is shown in Fig. 4. As a consequence, Eq. 9 is replaced by the following non-linear relationship (*cf.* Crémer *et al.* (2001), (2002)):

$$q_{M,0}^{el} = \pm \frac{Q_N}{\alpha K_{MM}} e^{-\varsigma Q_N} \qquad (11)$$

where $\zeta$ is a constant to be determined from experimental data (Chatzigogos *et al.*, 2008). If a purely frictional soil is considered, the three non-linear mechanisms are all active, with the difference that soil plasticity is no longer associated, and a plastic potential is introduced for the calculation of inelastic displacements.

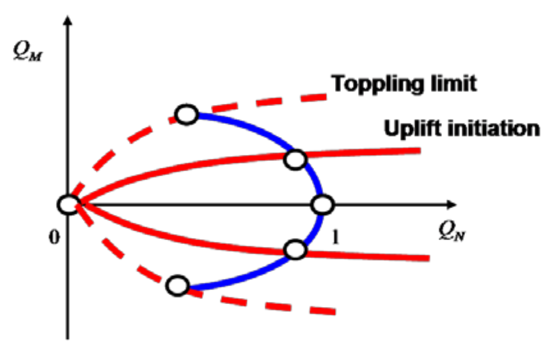


*Fig.4. Coupling between uplift and plasticity in the $Q_N$-$Q_M$ plane*

NUMERICAL APPLICATIONS

We herein illustrate some examples of results from the numerical tool presented in the previous section. Two circular bridge piers of different height have been chosen as representative cases of simple 1 dof systems. They have been designed (Restrepo, 2007) following the Direct Displacement Based Design methodology (Priestley *et al.*, 2007), and their main characteristics are shown in Table 1. The piers are modelled with an elastic perfectly plastic constitutive law for the superstructure, and three alternative conditions for the soil-foundation interaction, namely: fixed base, elastic base and elastoplastic base (for the third case both Paolucci and Chatzigogos macro-elements are implemented).

Table 1. Parameters of the examined piers

| **Quantity** | **Symbol** | **Unit** | **Pier P1** | **Pier P2** |
|---|---|---|---|---|
| Pier height | $h$ | [m] | 10 | 30 |
| Superstructure mass | $m_1$ | [t] | 882 | 1025 |
| Pier diameter | $D$ | [m] | 2 | 2.5 |
| Pier “cracked” stiffness | $K_1$ | [kN/m] | 25416 | 3048 |
| Pier yield displacement | $x_y$ | [m] | 0.085 | 0.614 |
| Footing width | $B$ | [m] | 7 | 8 |
| Footing mass | $m_0$ | [t] | 187.3 | 244.6 |
| Static bearing capacity | $N_{max}$ | [kN] | 65300 | 97440 |
| Footing safety factor | $FS$ | [-] | 5.8 | 6 |
| Footing rotational stiffness | $K_{MM}$ | [MNm] | 17640 | 26331 |

The piers square foundations rest on a frictional soil, characterized by a friction angle $\Phi$ = 32°, and by a shear modulus $G$ = 80 MPa. The static bearing capacity $N_{max}$ has been calculated following Eurocode 7 formulation, while foundation impedances have been computed using standard formulas used in practice (Gazetas, 1991). The two piers have been subjected to an accelerogram recorded during the Kocaeli earthquake (Turkey, 17/08/1999, $M_w$ 7.4), the displacement spectrum of which is similar to the Eurocode 8 displacement design spectrum (type 1, pga = 0.5g, soil C). The input signal is shown in Fig. 5.

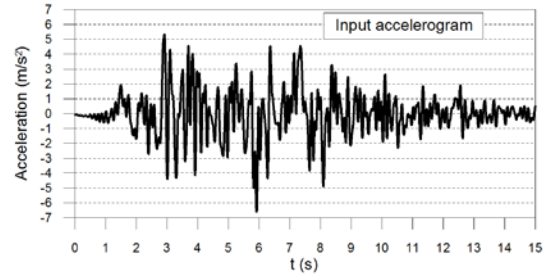


*Fig.5. Input accelerogram considered for the dynamic analyses, from the 17/08/1999, $M_w$ 7.4, Kocaeli earthquake*

Figure 6 presents a comparison between the results obtained from dynamic analyses performed on pier P1, considering different base conditions. The fixed base structure develops a ductile behaviour, with a peak lateral displacement of 26cm and a permanent displacement of 12cm. The consideration of a linear elastic soil-foundation interaction, causes an increase of the peak and permanent total lateral displacements of the system up to 37cm and 25cm respectively, with a negligible contribution of foundation rotation on the total displacement of the system. This implies that the structural ductility increases from the fixed base case to the linear soil-structure interaction case. The third considered base condition is described by the elastic perfectly plastic Paolucci macro-element. In this case, the total peak lateral displacement is equal to 34cm: 30cm due to the superstructure distorsion, and 4cm due to the foundation rotation. The structural ductility increases with respect to the fixed base case, but it decreases with respect to the linear interaction. Also the permanent displacement decreases with respect to the linear base case, up to a value of 17cm. In the left column of Fig. 6 the hysteretic cycles developed by the Paolucci macro-element foundation and by its elastic perfectly plastic superstructure are shown.  We observe that both the superstructure and the foundation enter into the non-linear range, developing plastic deformations and dissipating energy, although the superstructure gives the greatest contribution. Finally the elastoplastic base condition with uplift, described by Chatzigogos macroelement, is examined. In this case the total peak displacement is 32cm, a value close to that obtained in the previous case. However, the proportion between the contributions of the superstructure and of the foundation is different: the lateral structural distorsion is equal to 22cm, and the lateral displacement due to foundation rotation is around 10cm. This increase of foundation rotation causes a decrease of the structural ductility with respect to all previous base conditions, including the fixed base case. In the right column of Fig. 6 we can observe the hysteretic behaviour of Chatzigogos macro-element foundation and of its superstructure. We note that the reversible and non-dissipative uplift mechanism is dominant with respect to the plastic behaviour, which prevents the permanent plastic rotations of the foundation. In addition, also permanent structural distorsion is prevented, as the uplift mechanism tends to partially isolate the superstructure. The result is that the system approximately returns to its initial configuration, with negligible total permanent displacements.

The results of the dynamic analyses performed on the taller pier P2 are shown in Fig. 7. The peak displacement of the fixed base case is around 85cm. The superstructure develops plastic displacements, since its yield displacement is 61.4cm; the structural ductility is 1.38. Considering a linear elastic soil-foundation interaction, the total displacement of the system decreases, up to around 70cm: 60cm due to structural distorsion and 10cm due to foundation rotation. The superstructure remains in the elastic field, although close to the yield limit. The results from the Paolucci macro-element base case show an inversion between the contributions of superstructure and foundation to the total lateral displacement. The peak structural distorsion is around 30cm, while the displacement due to foundation rotation is larger, around 38cm. The total lateral displacement is 60cm; it is not given by the sum of the peak structural and foundation displacements, since they are not exactly in phase. It is noted that the foundation behaviour is highly non-linear, and the peak rotation nearly coincides with the permanent one.

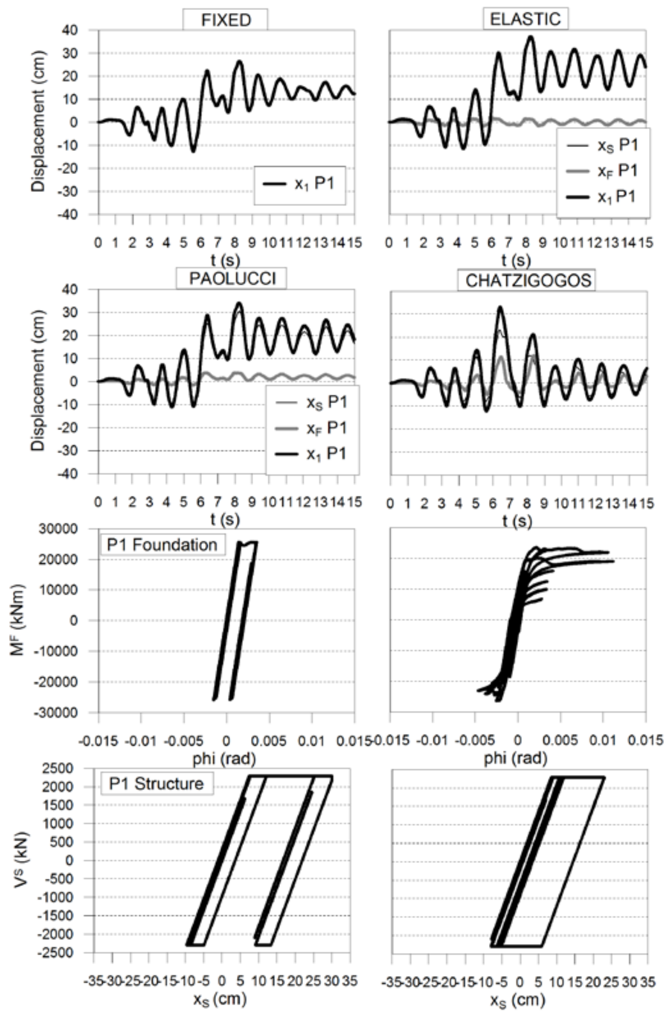


*Fig.6. Results obtained for pier P1 and different base conditions*

This is clear by observing the hysteretic cycle relative to the foundation, in the left column of Fig. 7: the peak and permanent foundation rotations are both close to 0.012radians. From the force-displacement plot relative to the superstructure, we note that it remains in the elastic field, with a peak base shear of 1500kN. If we compare this value with the one obtained for the fixed base case as $V_b = K_1 \, x_y$ = 1871kN, we observe that there is a significant reduction in the base shear, around 20%. The last base condition, described by the elastic plastic macro-element with uplift, gives similar results as in the previous case, except for the foundation behaviour. The superstructure has a peak lateral displacement of 30cm, and a peak base shear of 1500kN. The foundation develops a peak rotation of around 0.016rad, which corresponds to a lateral displacement of 50cm. An important remark is that the foundation does not accumulate permanent rotations, as it is clear from its hysteretic behaviour (*cf.* right column of Fig. 7). This means that the uplift mechanism is dominant with respect to plasticity, and it provides a reversible behaviour of the system.

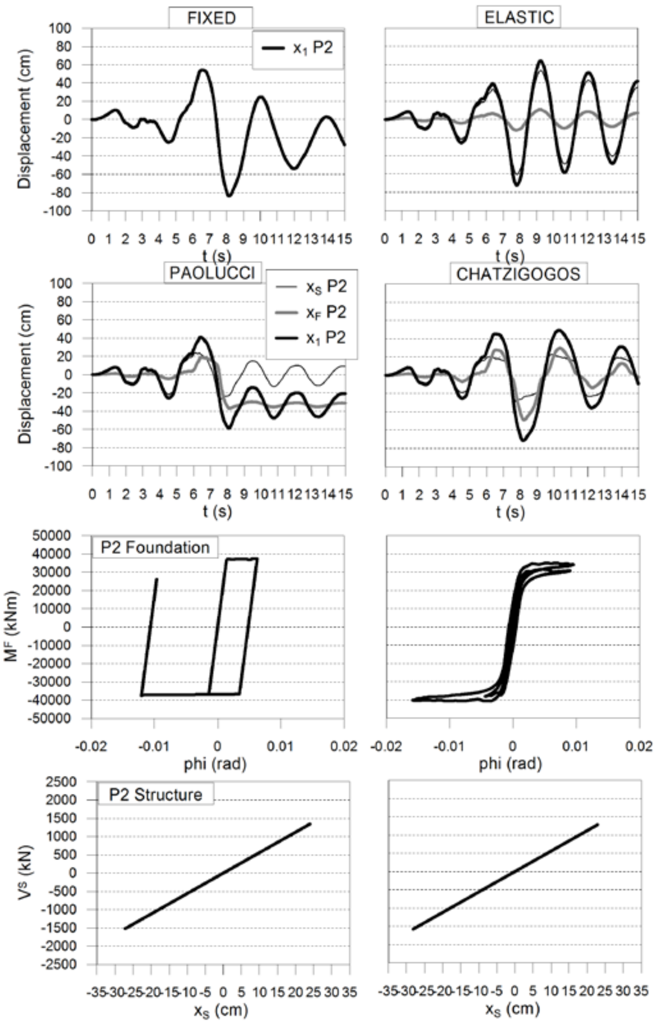


*Fig.7. Results obtained for pier P2 and different base conditions*

Comparing the results obtained for the two piers, we observe that the effects of non-linear soil-foundation interaction are more relevant for the higher pier P2. In this case the height and the flexibility of the pier provide a low base shear and a high moment acting on the foundation. As a consequence, more significant plasticization is produced at the soil-foundation level: this energy dissipation mechanism contributes to isolate the superstructure, which in fact remains in the elastic field. On the contrary, pier P1 is more rigid and lower: the base shear is higher and the moment on the foundation is lower than in pier P2. As a consequence, the plasticization is concentrated on the superstructure, and the non-linear soil-foundation interaction plays a minor role, providing a partial reduction of the structural ductility if the uplift mechanism is taken into account.

It is worth noting that this tendency is opposite to what would be expected from a linear elastic soil-structure interaction. It is well known that in this case the interaction effects increase as the rigidity of the structure increases, and as its heigth decreases.

## CONCLUSIONS

In this paper we have presented a simple numerical tool for non-linear dynamic soil-structure interaction analyses, based on the macro-element concept. After the presentation of the mathematical formulation of the tool, and the description of the two macro-element models implemented in it, we have shown some results obtained by dynamic analyses performed on bridge piers. The proposed numerical applications clearly point out the importance of characterizing properly the base condition of structures in soil-structure interaction analyses. We have observed that the system response can significantly change passing from a fixed base to a flexible base. Relevant differences appear also comparing alternative descriptions of soil-structure interaction: elastic, elastic perfectly plastic, or elastic plastic with uplift. In particular the role of non-linear interaction reveals its importance, since a dissipation mechanism can develop at the foundation level, acting as an isolator with respect to the superstructure. The non-linear mechanisms envisaged in this paper tend to emphasize the two basic aspects of the response of the foundation system, either dominant plastic dissipation (Paolucci model) or dominant uplift (Chatzigogos model). Studies are in progress to improve the coupling of both mechanisms.

We believe that the presented numerical tool will constitute a practical yet accurate tool for assessing the importance of each source of non-linearity in performance-based design procedures with account of non-linear soil-structure interaction.

## REFERENCES


Bransby, M.F., Randolph, M.F. [1998]. “Combined loading of skirted foundations”, Géotechnique, No. 48, pp. 637-655.

Chatzigogos, C.T. [2007]. “Comportement sismique des fondations superficielles: Vers la prise en compte d’un critère de performance dans la conception” (in French), *PhD Thesis*, École Polytechnique, Palaiseau, France.

Chatzigogos, C.T., Pecker A., Salençon, J. [2008]. “Macroelement modeling of shallow foundations”, Soil Dynamics and Earthquake Engineering, No. 29, pp. 765-781.

Chatzigogos, C.T., Figini, R. [2008]. “A general macroelement for shallow foundations and applications for performance-based design”, *Proc. 19th European Young Geotechnical Engineers’ Conference, 3-5 September 2008,* Gyor, Hungary

Crémer, C., Pecker, A., Davenne, L. [2001]. “Cyclic macro-element for soil-structure interaction: material and geometrical non linearities”, International Journal for Numerical and Analytical Methods in Geomechanics, No. 25, pp. 1257-1284.

Crémer, C., Pecker, A., Davenne, L. [2002]. “Modelling of nonlinear dynamic behavior of a shallow strip foundation with macroelement”, Journal of Earthquake Engineering, No. 6, pp. 175-211.

Dafalias, Y.F., Hermann, L.R. [1982]. “Bounding surface formulation of soil plasticity. Soil Mechanics – transient and cyclic loading”, Pande, G. N., Zienkiewicz, O. C., Eds., Wiley, pp. 173-218.

Gazetas, G. [1991]. “Foundations Vibrations”, in *Foundation Engineering Handbook*, (H.Y. Fang, ed.) Van Nostrand Reinhold, New York, NY, pp. 553-593.

Gouvernec, S. [2007a]. “Shape effects on the capacity of rectangular footings under general loading”, Géotechnique No. 57, pp. 637-646.

Gouvernec, S. [2007b]. “Failure envelopes for offshore shallow foundations under general loading”, Géotechnique No. 57, pp. 715-728.

Koiter, W.T. [1960]. “*Progress in Solid Mechanics*”, Vol. I, North Holland, Amsterdam, pp. 165-221.

Mandel, J. [1965]. “Généralisation de la théorie de la plasticité de W. T. Koiter”, International Journal of Solids and Structures, No. 1, pp. 273-295.

Nova, R., Montrasio, L. [1991]. “Settlements of shallow foundations on sand”, Géotechnique, No. 41, pp. 243-256.

Paolucci, R. [1997]. “Simplified evaluation of earthquake-induced permanent displacements of shallow foundations”, Journal of Earthquake Engineering, No. 1, pp. 563-579.

Paolucci, R., Shirato, M., Yilmaz, T.M. [2008]. “Seismic behavior of shallow foundations: shaking table experiments vs. numerical modeling”, Earthquake Engineering and Structural Dynamics, No. 37, pp. 577-595.

Prévost, J.H., Keane, C.M. [1990]. “Multi-mechanism elasto-plastic model for soils”, ASCE Journal of Engineering Mechanics, No. 116, pp. 1255-1263.

Priestley, M.J.N., Calvi, G.M., Kowalski, M.J. [2007]. “*Displacement-based seismic design of structures*”. IUSS Press, Pavia, Italy.

Restrepo, J.C.O. [2007]. “Displacement-based design of continuous concrete bridges under transverse seismic excitation”, *Master’s thesis*, European School for the Reduction of Seismic Risk, Pavia, Italy.

Salençon, J., Matar, M. [1982]. “Capacité portante des fondations circulaires”, Journal de Mécanique théorique et appliquée No. 1, pp. 237-267.

Wolf, J.P. [1988]. “*Soil-structure interaction analysis in the time domain*”. Prentice Hall Inc., New Jersey.

Wolf, J.P., Song, C. [2002]. “Some cornerstones of dynamic soil-structure interaction”, Engineering Structures, No. 24, pp. 13-28.